Overbounding Revisited: Discrete Error-Distribution Modeling for Safety-Critical GPS Navigation

Jason H. Rife and Boris Pervan
Tufts University

>> Accepted Article <<

CITATION:
J. Rife and B. Pervan, "Overbounding Revisited: Discrete Error-Distribution Modeling for Safety-Critical GPS Navigation," in *IEEE Transactions on Aerospace and Electronic Systems*, vol. 48, no. 2, pp. 1537-1551, April 2012.
doi: 10.1109/TAES.2012.6178077

CORRESPONDING AUTHOR:
Jason Rife
jason.rife@tufts.edu

FINANCIAL SUPPORT:
Federal Aviation Administration GBAS Program (FAA Contract DTFACT-15-C-00033)

Overbounding Revisited: Discrete Error-Distribution Modeling for Safety-Critical GPS Navigation

Jason Rife and Boris Pervan

***Abstract*—For a growing number of aviation applications of the Global Positioning System (GPS) and of other Global Navigation Satellite System (GNSS), it is essential to establish a rigorous bound on measurement error. Most existing bounding methods rely on representing the actual measurement error distribution with a conservative, continuous model (e.g., a Gaussian "overbound"). We propose a conservative, discrete model as a practical alternative. A key limitation of continuous error models is validation, particularly in the distribution tails where comparatively little statistical data is available. With a discrete model, it is easy (1) to define a minimally conservative core region, where data are plentiful, and (2) to introduce a highly conservative tail region, where data are sparse. The trade-off is increased computational complexity, as no closed-form expression exists for convolution of non-Gaussian error distributions. We propose a particular form of a discrete error distribution, which we call the NavDEN model. Through application to a heavy-tail GPS data set, we demonstrate that the NavDEN model compares favorably to Gaussian models, both in providing more margin for tail uncertainty and, at the same time, in providing generally tighter protection levels when multiple distributions are convolved.**

Keywords: GPS, GNSS, GNSS Augmentation, GBAS, SBAS, Overbounding

This work is based on the paper "Overbounding Revisited: Toward a More Practical Approach for Error Modeling in Safety-Critical Applications," presented at ION GNSS 2009, Savannah, GA, September 2009.

The authors gratefully acknowledge the Federal Aviation Administration Satellite Navigation Services, GBAS Program Office for supporting this research. The constructive comments and advice provided by Todd Walter, Juan Blanch, and Grace Gao are greatly appreciated. The opinions discussed here are those of the authors and do not necessarily represent those of the FAA or other affiliated agencies.

Authors' current addresses: J. Rife, Dept. of Mechanical Engineering, Tufts University, Medford, MA 02155, E-mail: (jason.rife@tufts.edu). B. Pervan, Dept. of Mechanical, Materials, and Aerospace Engineering, Illinois Institute of Technology, Chicago, IL 60616.

I. INTRODUCTION

This paper presents a method for evaluating a GNSS positioning-error bound. Our method has potential to streamline certification for new navigation systems and augmentations critical for Air Traffic Management (ATM), by reducing the amount of data needed to characterize distribution far tails and by establishing an error bound that is both tighter and more rigorous than what is possible using a more conventional Gaussian error model. New navigation technologies are needed to support plans for the Next Generation Air Transportation System (NextGen) in the United States and the Single European Skies ATM Research (SESAR) initiative in Europe [1,2]. These plans will dramatically realign ATM operations, enabling the airspace to double or triple its capacity by 2025. To accomplish this goal, without sacrificing safety, future ATM will make extensive use of four-dimensional (4D) trajectories, which describe an aircraft's flight plan not only in terms of its ground track and altitude, but also in terms of waypoint arrival times [3,4]. A complete 4D trajectory will define the entire space-time path of an aircraft from its departure gate (through takeoff, en route travel, approach and landing) to its arrival gate. Aggressive new sensing capabilities will be required to enable precise, 4D navigation with guaranteed separation between aircraft.

A. Motivation

Improved validation methods are needed to streamline certification of new navigation systems. Currently, verification and validation activities consume the majority of the time and capital investments required to field a new navigation system. These massive investments are driven in large part by the aggressive limits placed on *integrity risk*, which is the risk that a navigation reading is subject to a large, undetected measurement error [5]. As an example, consider the Ground-Based Augmentation System (GBAS), which was certified by the Federal Aviation Administration (FAA) in 2009 to support Category I landing (down to 200 foot visibility). This operation requires a guarantee that integrity risk is less than $2 \cdot 10^{-7}$ per approach, meaning that a misleading position measurement occurs no more frequently than once in ten million landings. The requirement for Category III (zero visibility landing) will be an integrity risk of less than 10^{-9} per approach [6].

Relating experimental error data to theoretical integrity bounds remains a key challenge for certifying safety-critical navigation systems. In particular, validating integrity risk is difficult because existing integrity analyses rely on continuous, Gaussian probability density models which are not necessarily justified by experimental data. This

reliance is motivated by the remarkable properties of Gaussian distributions, which benefit practical implementation, simplifying the communication and computation of error bounds used to assess integrity on-the-fly in avionics.

This paper's central contribution is the introduction of a particular discrete distribution, labeled the Navigation Discrete ENvelope (NavDEN) model, which provides a rigorous paired overbound for measurement error, one which is Gaussian at its core and non-Gaussian in its tails. Importantly, the NavDEN is designed to make the error model more suitable for safety-of-life navigation applications with constrained communication and computational resources. The paper will focus in particular on validation, communication and computation issues for GNSS augmentation systems such as GBAS as well as SBAS (Space Based Augmentation Systems), a category which includes WAAS in the United States and EGNOS in Europe.

B. Background

In GNSS augmentation systems, communication and processing constraints have motivated a nearly universal reliance on Gaussian error modeling. Unbiased Gaussian distributions are described by a single parameter: the standard deviation, sigma. The bandwidth for GBAS (or for SBAS) is just sufficient to transmit this single-parameter for each GPS satellite. By contrast, discrete distribution models generally employ a great many parameters, making them less suitable for broadcast. Gaussian distributions also offer an advantage in that a closed-form equation exists to describe the total contribution of independent, Gaussian error sources to the aircraft position estimate. No compact, closed-form solution exists for computing the position-error distribution when the summed measurement errors are distributed in a non-Gaussian fashion. Thus, practical engineering constraints on both communication and computation favor the use of Gaussian error models in navigation applications.

An overreliance on Gaussian distributions makes formal validation difficult, since actual error distributions cannot necessarily be conservatively bounded by a Gaussian [7]-[9]. To facilitate more rapid, more rigorous validation, this paper proposes an alternative to the continuous Gaussian-distribution error model. Specifically, we define a discrete distribution model that is both tighter (more accurate) than conventional models in the distribution core and looser (more tolerant of uncertainty) in the far tails. This approach was developed in parallel with an alternative method for discretely bounding error distributions [10]; the alternative method is easier to apply, but makes more restrictions on the form of the actual error distribution (e.g. the actual distribution must be symmetric and have only a single, global peak).

Our proposed approach for discrete error modeling builds on two Cumulative Distribution Function (CDF) overbounding concepts: paired overbounding [11] and core overbounding [9]. The term *overbounding* is typically used to describe the process of assuring integrity risk by relating error models for individual measurements to the error model for the combined GNSS position solution. Originally introduced in [12], CDF overbounding is widely used in navigation system validation, as this method can be used to show that a conservative position-error distribution can be computed from a set of conservative measurement-error distributions. Early CDF overbounding methods were valid only for a restricted class of distributions (independent, zero-mean, symmetric, and unimodal). Paired overbounding is a generalization of CDF overbounding that ensures integrity for arbitrary independent distributions by introducing both lower and upper bounds for a distribution (paired bounds). This technique is particularly useful in validating bounds for real error distributions, which are often asymmetric or biased [13]. Core overbounding further generalizes CDF overbounding to cover heavy-tail error distributions by allocating a nonzero probability for very large errors (approaching infinity). This approach addresses a critical issue in validating GNSS error models, since experiments indicate that large errors do occur with a greater than Gaussian frequency, even though nominal GNSS errors are distributed in an essentially Gaussian manner [14]. However, the basic core bounding approach (based on a Gaussian model) is too conservative to be used in practical applications.

In constructing a discrete distribution model for actual errors, it is desirable to retain the useful properties of these existing overbounding methods. In particular, we seek a discrete distribution model that uses upper and lower bounds, in the manner of paired bounding, so that the methodology can be applied to arbitrary independent distributions. Moreover, we seek to a method that can bound arbitrary distribution tails (heavy or truncated), in the spirit of core overbounding, but without relying on the excessively conservative measure of assuming that a non-negligible fraction of errors may be infinitely large. Our proposed solution is to introduce an error bound based on discrete intervals of bounded probability. By design, these intervals are small in the distribution core and wider in the distribution tails, where uncertainty is greatest.

It is instructive to note that the concept of representing an error distribution as a set of finite probabilities defined over discrete intervals is an idea that has previously been explored in the computational probability literature [15]-[17]. No prior effort has been made, however, to adapt these methods to aviation applications. Interval-based probability models, also called discrete envelope (DENV) methods, generally characterize each interval by three parameters: a right bound, a left bound, and a finite probability. As an example, a DENV model for a Gaussian

distribution is illustrated in Figure 1. In the figure, the height of each envelope corresponds to a probability. The left and right edges of each envelope define the associated interval. As with conventional error distributions, the total probability over all envelopes sums to unity. The specific distribution of errors within each envelope, however, need not be known or modeled.

Although conventional DENV models apply only to independent distributions, continuing research has sought to generalize these methods for application to correlated errors [18], which are important to a number of aviation applications [19]-[20]. Although such a generalization appears feasible, this paper will focus specifically on modeling independent measurement errors.

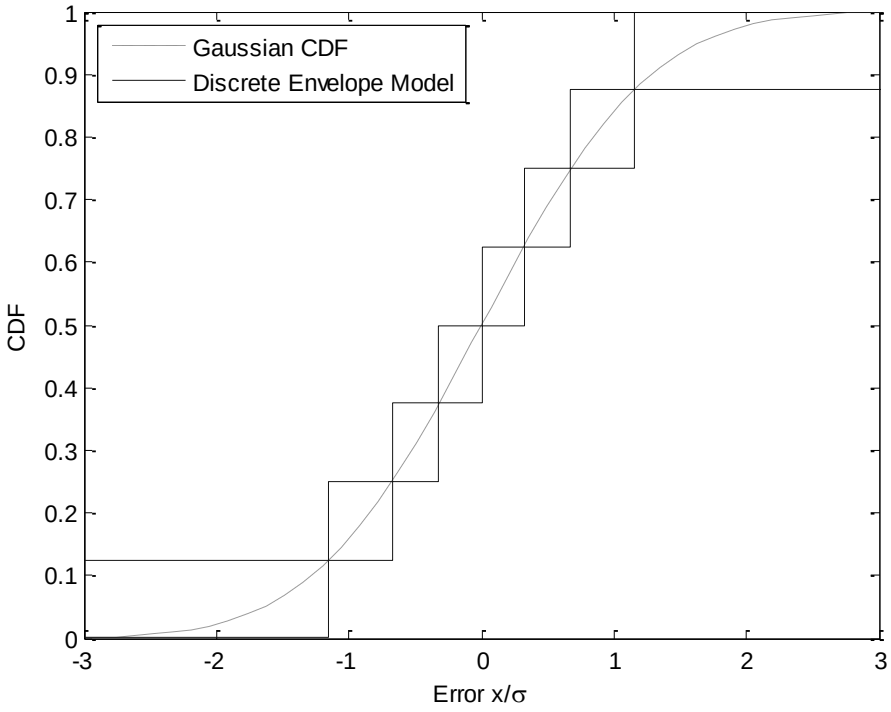

Figure 1. A Gaussian distribution represented by a DENV model consisting of eight envelopes.

The remainder of the paper describes a discrete-envelope approach tailored for navigation integrity applications. The next section details the structure and parameters of our proposed model, which we call the NavDEN distribution. Subsequently, we discuss (1) experimental model validation, (2) efficient communication, and (3) computation of a position-error bound. An analysis is conducted to demonstrate that even a highly

conservative NavDEN model for the distribution far tails can result in reduced inflation as compared to a conventional Gaussian bound (when multiple error sources are convolved). A final section summarizes significant results.

II. NavDEN: A Discrete Error Model for Integrity Applications

Experiments which have collected large sample sets of GNSS error data (relative to a calibrated location) indicate that typical small and moderate GNSS errors are well represented by a Gaussian distribution. However, larger errors, beyond 2-3 sigma, occur with non-Gaussian probability [14]. For most systems, large errors occur with higher than Gaussian probability (heavy distribution tails). For a few systems, large errors appear to be absent altogether (truncated distribution tails).

To reflect these characteristics of GNSS measurement uncertainty, we propose an error distribution model, which we call the NavDEN. The NavDEN is a discrete model that approximates a Gaussian in its core but that flares in its tails, to enable bounding both of truncated and of heavy-tail distributions. The shape of the NavDEN CDF model is illustrated in Figure 2. In the figure, probability is mapped to Gaussian coordinates, such that a Gaussian CDF is a straight line. This transformation converts a conventional CDF $P(x)$ to a Gaussian-quantile form $G(x)$ by mapping through the inverse of the Gaussian cumulative distribution $Q(x)$.

$$G(x) = Q^{-1}\left(P(x)\right) \quad (1)$$

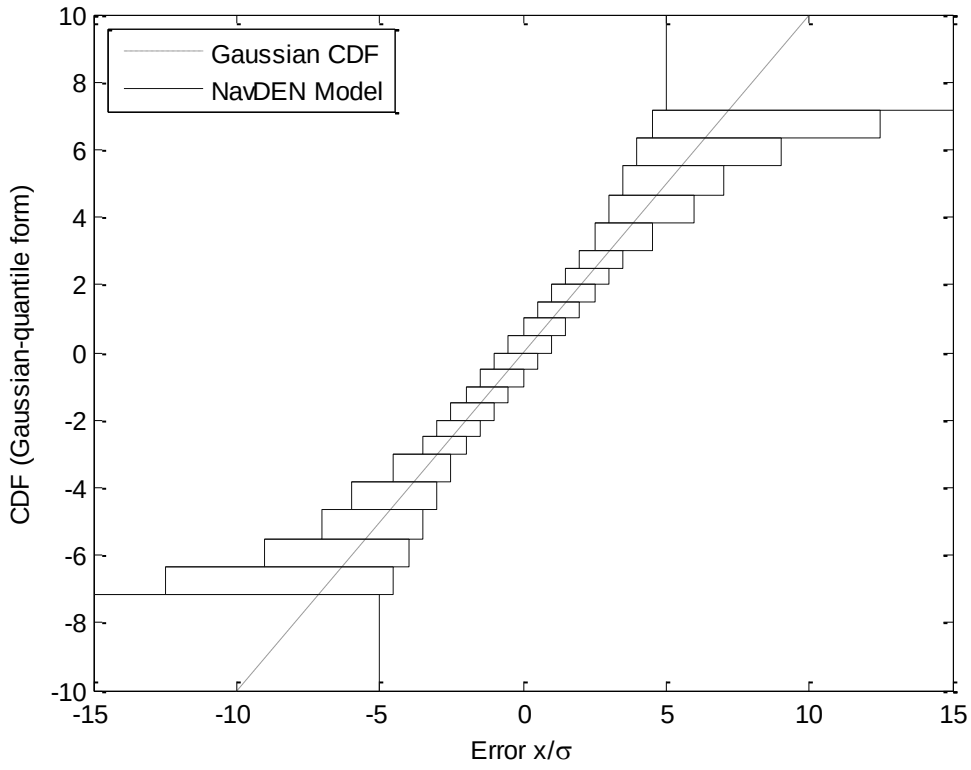

Figure 2. The NavDEN model plotted on Gaussian-quantile axes.

The structure of the NavDEN ensures efficient communication and computation, as will be described in subsequent sections. Salient features of the NavDEN structure, which can be observed in the figure, include:

- The envelope distribution is symmetric.
- Probability is not distributed uniformly among the envelopes.
- Envelope widths are non-uniform, with width increasing toward the distribution tails.
- Envelope edges fall on a regularly spaced grid, at integer multiples of a baseline spacing Δ.

A key feature of the NavDEN distribution is the transition between the well-characterized, approximately Gaussian core and the more uncertain tail region. To represent this transition, the NavDEN model uses three regions: a flared tail describing large negative errors, an approximately Gaussian core, and a second flared tail describing large positive errors. Each of these three regions (K_1, K_2, and K_3 respectively) consists of a subset of envelope boundaries, enumerated below using the integer index k.

$$K_1 = \{k \in [k_{\min}, -k_{tr})\}$$
$$K_2 = \{k \in [-k_{tr}, k_{tr}]\} \qquad (2)$$
$$K_3 = \{k \in (k_{tr}, k_{\max}]\}$$

Here k_{max} is the largest index, k_{min} is the smallest index, and k_{tr} is the index that demarcates the transition between the Gaussian core (K_2) and the positive tail region (K_3). In this paper, we set the upper and lower indices to be nearly equal in magnitude $(k_{\min} = -k_{\max} - 1)$.

The shape of the NavDEN model is defined by a set of six additional parameters. The most important parameter is the fundamental grid spacing Δ, which determines the resolution of the NavDEN model. Four more parameters determine the shape of the flared regions which bound large errors. A final parameter determines the lateral offset between the left and right bounds in the distribution core.

The parameters that control tail shape include two asymptote parameters and two curvature parameters. As shown in the figure, the inside edges of the NavDEN converge toward a vertical asymptote. Similarly, the outer edges converge toward a horizontal asymptote. The parameters are x_{max} (vertical asymptote) and x_{min} (horizontal asymptote). The existence of a vertical asymptote allows the NavDEN to accommodate truncated distributions, and the existence of the horizontal asymptote, to accommodate heavy-tail distributions. One curvature parameter, *B*, governs how quickly the inner edge of the NavDEN transitions to the vertical asymptote. A second curvature parameter, *C*, governs how quickly the outer edge of the NavDEN transitions to the horizontal asymptote. In the following discussion, these parameters will be described using a tilde notation $(\tilde{x}_{\max}, \tilde{x}_{\min}, \tilde{C}, \tilde{B})$, where the tilde indicates a unitless ratio of each parameter over the fundamental spacing.

The left and right bounds of the NavDEN are offset away from zero. The offset magnitude, normalized by the fundamental spacing, is labeled k_{bias}. This offset allows the NavDEN to bracket the confidence bounds on either side of an empirical cumulative probability distribution (see Section VI). This offset also allows the actual distribution to be mildly biased, asymmetric and/or multimodal [11].

The normalized left bound $\tilde{l}_k$ of the NavDEN is given by the following equation. In this equation, all parameters have been normalized by the fundamental spacing Δ.

$$\tilde{l}_k = \begin{cases} \text{floor}\left(\tilde{C} \ln\left(1 - \dfrac{k + k_{tr}}{k_{\min} + k_{tr}} \right) - k_{tr} - k_{bias} \right), & k \in K_1 \\ k - k_{bias} \ , & k \in K_2 \\ \text{floor}\left(\tilde{x}_{\max} - k_{bias} - \left(\tilde{x}_{\max} - k_{tr} \right) e^{2(k_{tr} - k)/\tilde{B}} \right), & k \in K_3 \end{cases} \qquad (3)$$

The "floor" operator ensures regular spacing by rounding conservatively outward to the nearest integer multiple of Δ. This equation was designed to transition continuously (in value) from the Gaussian core, through the curved tail regions, and toward the desired asymptotes. The equation is also continuous in slope, if $\tilde{B} = \tilde{x}_{\max} - k_{tr}$ and $\tilde{C} = -\left(\tilde{x}_{\min} + k_{tr} \right)$; however, greater flaring is possible by increasing $\tilde{B}$ and $\tilde{C}$ from these baseline values.

Each left edge is associated with a particular cumulative probability value. Within each region (negative flare, core, positive flare), these cumulative probability values are spaced at even Gaussian quantiles.

$$\underline{\tilde{G}}_k = \begin{cases} -k_{tr} + \psi_1 \left(k + k_{tr} \right) & k < -k_{tr} \\ k & -k_{tr} \le k \le k_{tr} \\ k_{tr} + \psi_3 \left(k - k_{tr} \right) & k_{tr} < k \end{cases} \qquad (4)$$

Here the underscore ($\underline{\tilde{G}}_k$) indicates that the probability is associated with the lower (left) boundary. The ψ_i terms are slopes for each region *i*. These slopes match the number of points in each region with the specified asymptote and transition parameters.

$$\psi_1 = \frac{\tilde{x}_{\min} + k_{tr}}{k_{\min} + k_{tr}}, \quad \psi_2 = 1, \quad \psi_3 = \frac{\tilde{x}_{\max} - k_{tr}}{k_{\max} - k_{tr}} \qquad (5)$$

The probability values in Gaussian quantile coordinates can be converted into conventional cumulative probabilities by inverting the *Q* function. It should be noted that the *Q* function is the CDF for a unit-variance Gaussian, but that the nominal standard deviation for the actual error distribution is $S_i \sigma_i$, where S_i is the geometric weighting factor for the i^{th} satellite and σ_i is the nominal standard deviation for the raw measurement data.

$$P(\Delta \tilde{l}_k) = Q\left(\frac{\Delta \underline{\tilde{G}}_k}{S_i \sigma_i} \right) \qquad (6)$$

The distribution of envelopes is symmetric about the origin. The normalized right-bound edges r_k and their associated cumulative probabilities ($\overline{\tilde{G}}_k$) can thus be obtained by evaluating these quantities in reverse order.

$$\tilde{r}_k = -\tilde{l}_{-k-1} \quad (7)$$

$$\overline{\tilde{G}}_k = -\underline{\tilde{G}}_{-k-1} \quad (8)$$

When the asymptotes occur symmetrically about the origin ($\tilde{x}_{\max} = -\tilde{x}_{\min}$), then the spacing of cumulative probabilities is the same on both sides of the flared tail ($\psi_1 = \psi_3$), and the number of envelopes is equal to the total number of indices. In this paper, we consider only the symmetric case; however, were the asymptotes asymmetric ($\tilde{x}_{\max} \neq -\tilde{x}_{\min}$), then the spacing of cumulative probabilities in either tail would also be asymmetric ($\psi_1 \neq \psi_3$), and so each left and each right edge would generate its own distinct envelope.

Table 1 summarizes the set of NavDEN parameters. The values of each parameter used to generate Figure 2 are also listed. Because this nominal standard deviation is different for each satellite (and is defined in real-time by the data link broadcast for existing augmentation systems including GBAS and SBAS), the fundamental spacing is defined as a multiple of the nominal standard deviation. In other words, the parameter is defined as a constant value, $\Delta_i = S_i \sigma_i$.

Table 1: Representative NavDEN Parameters

Parameter	Value
$\Delta_i / (S_i \sigma_i)$	**0.5**
$\tilde{x}_{\max}$	**16**
$\tilde{x}_{\min}$	**-16**
$\tilde{B}$	**10**
$\tilde{C}$	**10**
k_{tr}	**6**
k_{max}	**11**
$k_{\min}$	**-12**
k_{bias}	**1**

III. Characteristics of NavDEN Distribution

The NavDEN error model is specifically designed to promote efficient validation, communication and computation of integrity risk limits.

A. Validation

A major advantage of using a discrete envelope model is that it provides a robust framework for empirical validation. Given statistical uncertainty in sampled data [21], the precise form of the probability distribution cannot be known. For the NavDEN model to be conservative, the empirical CDF (or, more rigorously, its confidence bounds) must lie between the left and right distribution bounds. Because these bounds change in steps at discrete locations, the validation process requires that the empirical distribution be checked only at those locations.

Two sets of validation tests should be considered, one for left and one for right envelope edges. Expression for these tests can be written using the notation $H(x < X)$, which refers to an empirical CDF, computed by binning the number of samples (from a population of size C) whose value x does not exceed a threshold X. For envelope left bounds, the tests can be expressed as follows.

$$H\left(x < l_k\right) \leq C \sum_{i=-k_{tr}}^{k-1} p_i \quad (9)$$

A subsequent set of tests is used to validate envelope right bounds.

$$H\left(x \leq r_k\right) \geq C \sum_{i=-k_{tr}}^{k} p_i \quad (10)$$

The full suite of validation tests for the baseline NavDEN distribution is illustrated in Figure 3. Each circle represents a constraint imposed either by a right bound or a left bound. Empirical CDF values must lie along the dashed vertical lines. The dashed lines are longest where the NavDEN tolerates highest uncertainty (in the tails where the envelope overlap is greatest).

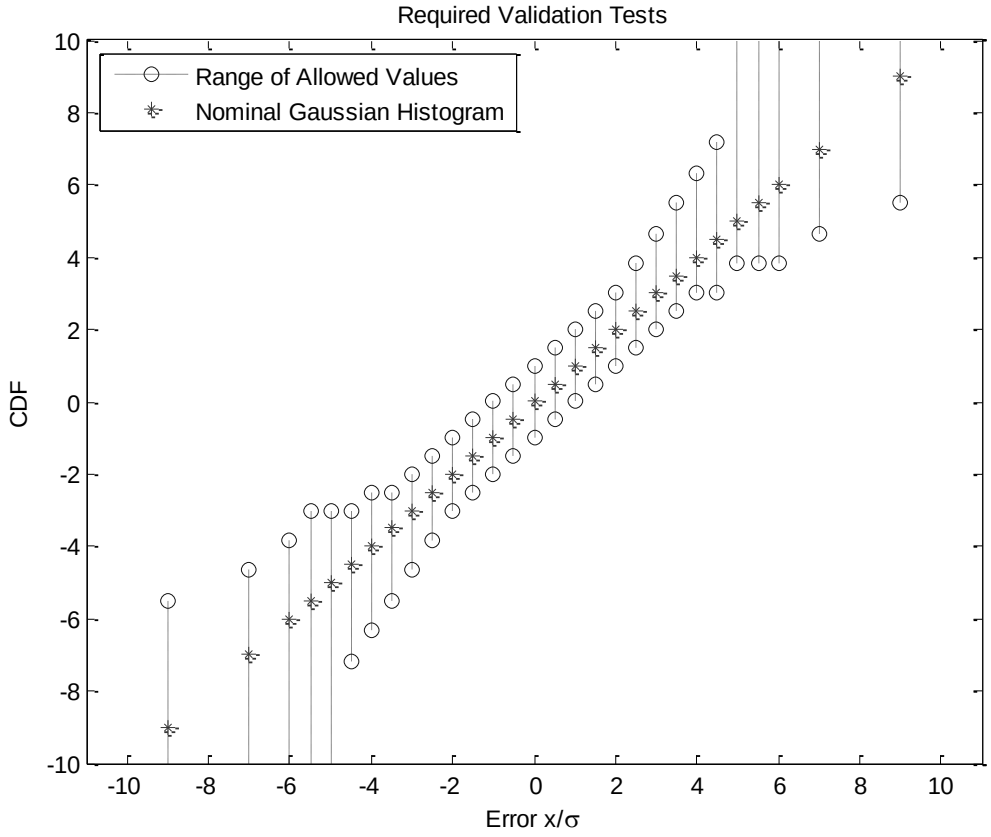

Figure 3. To validate the NavDEN model, the empirical CDF must fall in the range indicated by the vertical dashed lines.

It is significant to note that the right edge of any envelope should not be coincident with the left edge of the subsequent envelope. Were these two edges coincident, with no overlap such that l_k were equal r_{k-1}, then (9) and (10) could only be mutually satisfied for a single, precise value of the empirical CDF:

$$H\left(r_{k-1}\right) = H\left(l_k\right) = C\sum_{i=-k_{tr}}^{k-1} p_i \; . \quad (11)$$

It is for this reason that the NavDEN model (illustrated in Figure 2) is defined with overlapping envelopes (in contrast with the earlier discrete envelope example shown in Figure 1). Overlapping bounds allow for uncertainty in an empirical distribution function (which may be quantified, for example, by establishing 95% confidence bounds around the nominal distribution). Importantly, the NavDEN's flared tails increase the offset between the left and right bounds at the extremes of the distribution, aiding the NavDEN to tolerate high uncertainty in characterizing this region. A larger shift between the left and right bounds makes the validation process less sensitive to sampling noise

(which can otherwise plague validation [22]-[23]).

It is conceivable that the NavDEN tail parameters might be reconfigured over time, as a progressively larger population of validation data becomes available. In practice, the NavDEN tail flair should initially be set quite large, to account for possible truncated or heavy tails. Initial tail flare might be based, for instance, on expert opinion or on extreme value theory [24]. Distribution parameters, such as the *B* and *C* curvature parameters, might be later modified to reduce conservatism in the NavDEN tails. This potential to adapt the error model while the navigation system is in service offers significant potential to streamline navigation-system validation in the future. An application of the NavDEN to bound a particular GPS data set is described in Section VI.

B. Efficient Communication

The NavDEN structure permits the broadcast of concise error models via a limited bandwidth communication channel. At its heart, the NavDEN is an approximately Gaussian error distribution. In both the case of a conventional Gaussian and the case of a NavDEN, distribution width is defined primarily by a scaling parameter: the standard deviation ($S_i\sigma_i$) for a weighted Gaussian distribution or the fundamental spacing (Δ_i) for a NavDEN. It is largely for this reason that the fundamental spacing of the NavDEN is directly proportional to the standard deviation of the Gaussian distribution which the NavDEN approximates ($S_i\sigma_i$) as indicated in Table 1.

In this sense, the broadcast requirement is identical for either a Gaussian or a NavDEN overbound. Assuming the NavDEN parameters of Table 1 are known to all users (hard-coded in the avionics or transmitted via a very-low bandwidth communication channel), then only one variable need be broadcast in real-time to complete specification of the NavDEN model for each error source. This one parameter that must be transmitted in real-time is σ_i, the standard deviation of the Gaussian core for the i^{th} satellite error distribution. (The weighting parameter S_i is determined by the geometry of the satellites observed by any particular user.) In short, no change to the message types for existing navigation integrity systems, like WAAS or LAAS [25]-[26], would be needed to implement integrity assurance using the NavDEN distribution.

The compatibility of NavDEN error models with standard message definitions is a significant benefit. For full compatibility, it would be necessary to hard code the NavDEN parameters in user avionics. However, to maintain maximum flexibility during the validation process, we recommended that the complete set of NavDEN parameters be broadcast to users via a new low-rate message (once every several minutes). This would be necessary to enable

reconfiguration of the NavDEN parameters to reduce conservatism in the tails as more sampled data becomes available (see section III.B).

C. Computing Integrity Risk Limits - Protection Level

The ultimate use of NavDEN models is to enable users to assess integrity risk in order to determine whether or not to proceed with a safety-critical operation, such as precision approach or landing. A common means for checking integrity is to evaluate a *protection level* (PL), the smallest error magnitude beyond which the cumulative error probability might exceed the integrity risk specification [5]. The PL is compared to an *alert limit* (AL), the maximum allowable error for a particular operation. So long as the PL does not exceed the AL, the user may conduct the desired operation. Since position error varies with the specific set of GNSS satellites that any individual user views at any given time, it is not possible to pre-compute PLs. Rather, the PL must be assessed immediately before conducting a safety-critical operation.

In existing integrity systems, errors are modeled as Gaussian. For a purely Gaussian position-error distribution, the PL can be computed by inverting the unit-variance Gaussian CDF Q (at a specified risk R_{int}) and scaling by the position-error standard deviation in a particular axis σ_p.

$$PL = Q^{-1}\left(R_{\text{int}}\right)\sigma_p \quad (12)$$

The allowed integrity risk specification for aviation applications is generally miniscule. A representative value of R_{int} is on the order of 10^{-9}.

For GNSS position solutions, the error E_p along a particular axis is a linear combination of ranging measurement errors E_i, each weighted by a geometric scaling factor S_i for a particular satellite i [27].

$$E_p = \sum_{i=1}^{N} S_i E_i \quad (13)$$

Thus, if errors are Gaussian (with standard deviations σ_i), the position-error standard deviation σ_p is:

$$\sigma_p = \sqrt{\sum_{i=1}^{N} S_i^2 \sigma_i^2}\ . \quad (14)$$

Clearly, PL equations of the form of (14) are advantageous in that they provide a closed-form, computationally

efficient means to assess whether or not to proceed with a precision operation. However, such PL equations apply only to error sources that are well represented (or rigorously overbounded) by Gaussian distributions.

By comparison, the PL is somewhat more difficult to compute for measurement error distributions of non-Gaussian shape, including the NavDEN. For these cases, it is necessary to employ a numerical algorithm to compute PL. More precisely, a numerical convolution algorithm can be used (as long as measurement error distributions are independent). To perform discrete convolutions efficiently, it is essential that a uniform and consistent grid spacing be used for each pair of distributions being convolved. It is for this reason that the NavDEN distribution is defined on a regular grid based on a fundamental spacing Δ. It is important to note, however, that this spacing may not be the same for different GNSS satellites. As stated in the previous section, the "width" of each distribution is proportional to the standard deviation of the distribution core σ_i multiplied by a geometric weighting factor S_i, terms which vary from satellite to satellite. Accordingly, all but one satellite error distribution may need to be resampled in order to perform numerical convolution to compute the PL.

As a pre-processing step prior to each convolution, we recommend that the narrower of the two distributions be resampled. (That is the distribution with the smaller fundamental spacing should be resampled on to a grid defined by the larger fundamental spacing.) This downsampling procedure maintains or reduces the number of discrete envelopes output from the convolution operation. By comparison, upsampling the wider distribution (to a uniform grid based on the smaller fundamental spacing) might result in an arbitrarily large number of new discrete envelopes, which would result in unbounded time to compute the numerical convolution.

To maintain conservatism during downsampling, envelope right bounds must be rounded upwards (a ceiling operation) and left bounds must be rounded downwards (a floor operation). This method of downsampling ensures that formal left and right CDF-bounds can be constructed in a manner that ensures integrity [11]. For the narrower distribution, the downsampled right and left envelope bounds, $\breve{r}_k$ and $\breve{l}_k$, can be computed from the original right and left bounds (r_k and l_k), as follows.

$$\begin{aligned} \breve{r}_k &= \text{ceiling}\left(\frac{r_k}{\Delta_W}\right)\Delta_W \\ \breve{l}_k &= \text{floor}\left(\frac{l_k}{\Delta_W}\right)\Delta_W \end{aligned} \tag{15}$$

Here, the fundamental spacing of the wider distribution is given by the variable Δ_W. The above equation does not necessarily assign a probability to every point on the new grid. At points where no probability value is otherwise assigned, probability is set to zero. When the above equation assigns multiple envelope probabilities to the same point on the resampled grid, those probabilities are summed.

Once downsampling is complete, the numerical convolution can be computed as a conventional convolution of discrete distributions. Technically, paired bounding requires two convolutions – one to generate a new left bound and the other to generate a new right bound. In the case of the NavDEN, the right bound can be inferred from the left, because it is simply the reflection of the left distribution bound about the origin. For the left-bound, the convolution has the following form, where the narrow and wide distributions are labeled $\underline{p}_{N,k}$ and $\underline{p}_{W,k}$, respectively, and the output distribution is labeled $\underline{p}_k$.

$$\underline{p}_k = \sum_{l \in L} \underline{p}_{N,k-l}\, \underline{p}_{W,l} \qquad (16)$$

Here the set of all envelope indices in the wider distribution is labeled L. The right bound $\overline{p}_k$ is related to the left bound $\underline{p}_k$ by the following equation.

$$\overline{p}_{-k} = \underline{p}_k \qquad (17)$$

To evaluate the PL, discrete convolutions are repeated until each of the N satellite errors is factored into the position-error distribution (along a particular axis). Thus, N-1 discrete convolutions are required to evaluate the PL. Each of these N-1 convolutions calls for resampling, and each resampling step introduces mild additional conservatism. In resampling, the degree of overconservatism is larger when envelope edges are shifted farther. To keep these shifts small, it is recommended that each successive convolution be performed on the narrowest remaining distribution (i.e. the one with the smallest fundamental spacing). This algorithm is summarized below in Table 2.

Table 2: Algorithm to Obtain Position-Error Distribution for Multiple Independent Measurements

1. Sort NavDEN models for all measurements and assign an index i corresponding to the order of ascending fundamental spacing Δ_i.
2. Assign the left bound for the i[th] NavDEN to a distribution $\underline{{}^{(i)}f}_k$.
3. Initialize the position-error left-bound $\underline{p}_k$ by setting $\underline{p}_k = \underline{{}^{(1)}f}_k$.
4. For each index i (greater than one):
   a. Downsample $\underline{p}_k$ to the next fundamental spacing Δ_i.
   b. Update $\underline{p}_k$ by convolving it with the measurement error distribution $\underline{{}^{(i)}f}_k$:

$$\overline{p}_k = \sum_{l \in L} {}^{(i)}\overline{f}_l \cdot \overline{p}_{k-l}$$

The PL can be computed from the final convolved distribution. The PL corresponds to the grid point beyond which the total integrated probability is no more than the integrity risk allotment for the distribution tail (R_{int}). For a position-error distribution $\underline{p}_k$ this grid point is k[*]:

$$k^* = \max\left\{ k \;\middle|\; \sum_{i<k} \underline{p}_i \le R_{int} \right\}. \quad (18)$$

This dimensionless index can be converted to a PL when multiplied by Δ_{max}, the fundamental spacing of the final distribution (and also of the fundamental spacing of widest individual measurement-error distribution).

$$PL = \left| \Delta_{\max} k^* \right| \quad (19)$$

The absolute value operator accounts for the fact that the index k^* is generally a negative integer (on the left side of the origin), but that the PL is always reported as positive.

IV. Effect of Multiple Convolutions

One of the NavDEN's important features is that its tail flair diminishes with repeated convolutions. This analytical result could be anticipated as a consequence of the Central Limit Theorem, which states that most probability distributions become increasingly Gaussian when repeatedly convolved with themselves. Figure 4 provides an illustration of the NavDEN's convergence toward a Gaussian distribution following repeated convolutions. The left side of the figure depicts a baseline NavDEN distribution; the right-hand side depicts the result of convolving together ten independent, identical distributions (IIDs). In both cases, the NavDEN cumulative distribution functions are plotted using Gaussian quartile scaling, in which Gaussian distributions appear as straight lines. The nearly straight right and left bounds illustrated in Figure 4(b) are clearly indicative that repeated convolutions result in a pair of distributions that are very nearly Gaussian. These nearly straight paired bounds stand in stark contrast to the original NavDEN distribution, illustrated in Figure 4(a).

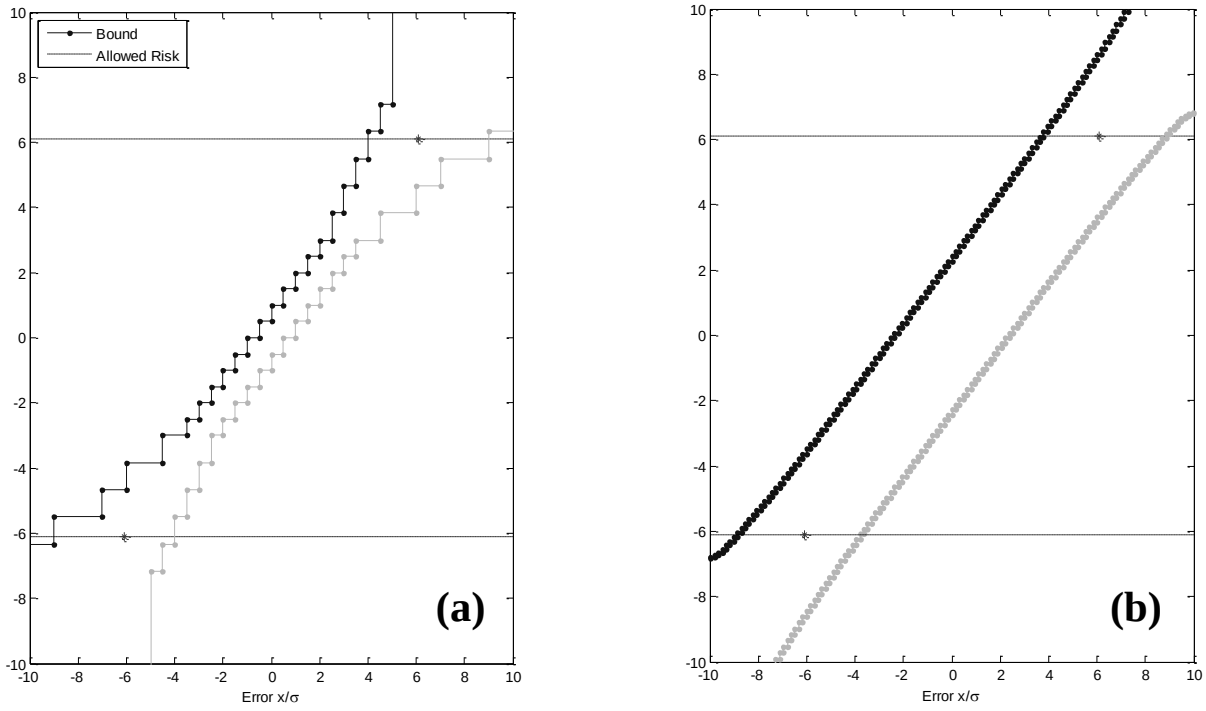

Figure 4. Assessing a protection level using the NavDEN model for (a) the case of one measurement and (b) the case of ten identical, independent NavDEN distributions

That heavy-tail distributions become increasingly Gaussian with repeated convolutions is a potential benefit, because heavy tails would otherwise further increase the PL, an effect which tends to reduces availability [28]-[29]. This benefit cannot be realized using a conventional Gaussian error model, which inflates the Gaussian sigma in an attempt to bound heavy tails [30]. When Gaussians are convolved, the output remains Gaussian, hence the level of inflation is fixed regardless of the number of convolutions performed. By contrast, the NavDEN directly models non-Gaussian tails, so the benefits of heavy-tail mitigation through convolution can be realized, providing the NavDEN with a potentially significant availability benefit.

This NavDEN benefit is partially offset by a negative effect: the growth in the bias between the left and right NavDEN edges that occurs with repeated convolutions. The left and right bound edges were intentionally offset to ensure tolerance for confidence intervals around the nominal empirical distribution (see Figure 2). Though this offset is necessary for validation, it is somewhat detrimental in that it increases PL and potentially decreases availability. Biases accumulate when NavDEN distributions are convolved, causing the effect of the bias to become increasingly pronounced when multiple error sources are combined. If a single distribution is offset by a bias b, then the convolution of N IIDs results in a bias equal to Nb. By comparison distribution standard deviation grows less rapidly (as the square root of N for a set of N convolved Gaussians, for instance). For N Gaussian IIDs, each with a bias b and a standard deviation σ, the formula for the PL is the following [11].

$$PL = Q^{-1}\left(R_{\text{int}}\right)\sqrt{N}\sigma + Nb \quad (20)$$

As N grows, the bias term of this PL equation becomes increasingly dominant. These opposing effects of heavy-tail mitigation and bias accumulation are visible in Figure 4.

For a typical number of satellites in view (4-10), the tradeoff between heavy-tail mitigation and bias accumulation provides a net benefit for the NavDEN model. This net benefit is illustrated in Figure 5. The figure plots the PL ratio ξ as a function of the number of IIDs convolved. The PL ratio is equal to the NavDEN PL normalized by the PL for a conventional Gaussian with the same core sigma. The ratio ξ is computed as follows.

$$\xi = \frac{\left|\Delta_{\max} k^*\right|}{Q^{-1}\left(R_{\text{int}}\right)\sqrt{N}\sigma} \quad (21)$$

The ratio ξ was computed for three different integrity risk levels (10^{-6}, 10^{-9}, and 10^{-12}). In order to minimize grid discretization effects (described in the next section), the number of discrete envelopes was increased above that of the baseline NavDEN illustrated in Figure 1. Specifically, the number of envelopes was set to eight times the baseline number.

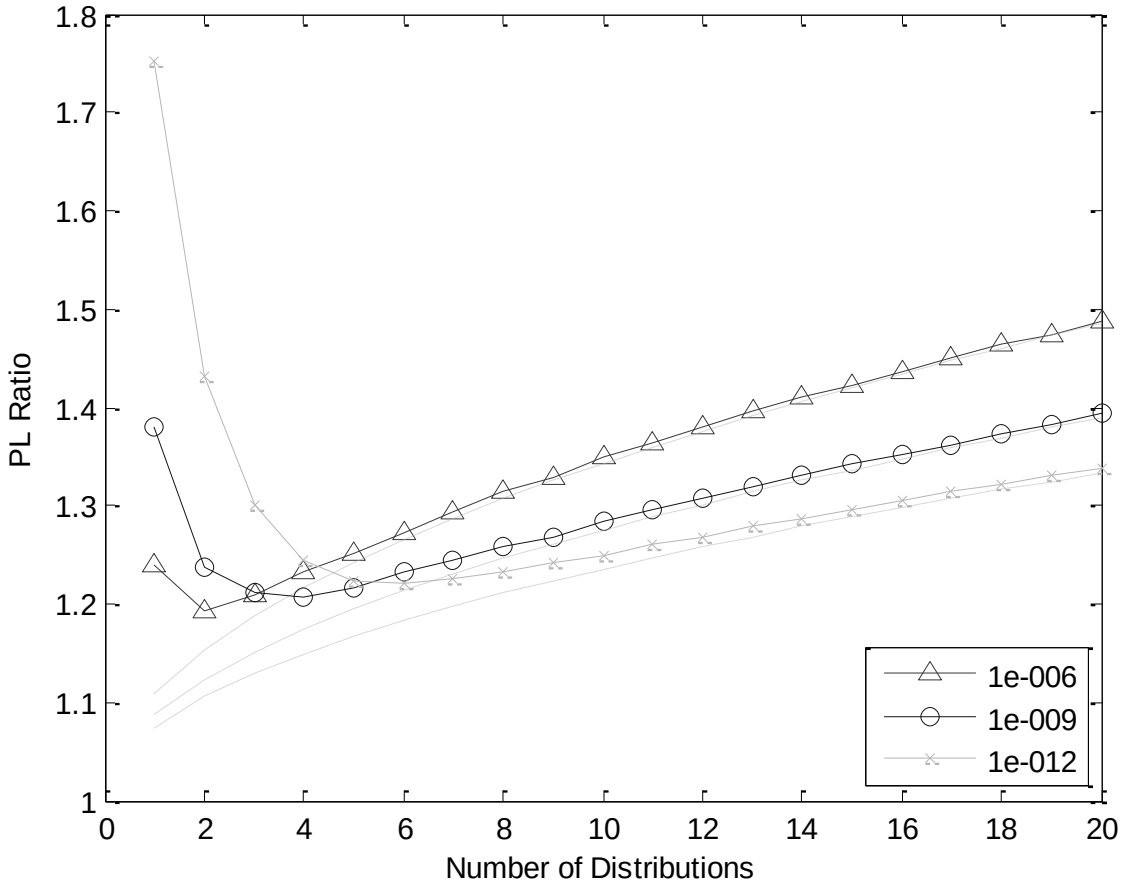

Figure 5. PL Ratio (for NavDEN as compared to Gaussian of same sigma) for various allocations of integrity risk

In the figure, it is evident that the lowest PL ratio occurs for a number of IID convolutions that falls between two and five (depending on the integrity risk level). Beyond this point, bias accumulation becomes increasingly significant. After a sufficient number of convolutions (ten or more), the benefits of heavy-tail mitigation are essentially cancelled by the detrimental effect of bias accumulation.

Moving toward the right-hand side of the plot, the NavDEN PL converges toward the PL for biased Gaussian IIDs (with no heavy tails). To show this, the PL ratio for convolution of biased Gaussian distributions is also plotted (dashed curves). These reference curves, ξ_{ref}, are a ratio of the biased Gaussian PL, from (20), to the PL for an unbiased Gaussian distribution, from (14).

$$\xi_{ref} = \frac{Q^{-1}\left(R_{\text{int}}\right)\sqrt{N}\sigma + Nb}{Q^{-1}\left(R_{\text{int}}\right)\sqrt{N}\sigma} \quad (22)$$

The fact that the NavDEN PL converges to the biased-Gaussian PL as the number of convolved IIDs becomes large underscores the decreased significance of heavy tails and the increased significance of the accumulated bias when the number of convolved IIDs is large.

V. Effect of Grid Resolution

Whereas the NavDEN intentionally introduces inflation to bound heavy tails and statistical uncertainty, the NavDEN also introduces an unintentional inflation source: inflation due to grid resolution. The discrete nature of the NavDEN distribution is both an advantage and a disadvantage. A coarse grid with fewer discrete envelopes reduces the computational costs for convolution and reduces the number of tests required for validation However, a coarser grid is limited by the conservative assumption that all probability in a given discrete envelope might, in the worst case, be assumed to lie at an envelope edge. When grid resolution is low, and discrete envelopes are wide, this worst case condition is much more detrimental to availability.

A grid resolution study was performed to determine the sensitivity of the PL to the number of envelopes in the NavDEN. The baseline NavDEN distribution (defined by the parameters in Table 1 and illustrated in Figure 2) has 23 envelopes. Three other cases were also generated by successively doubling the grid resolution, including a “2x” case (with 47 envelopes), a “4x” case (with 95 envelopes) and an “8x” case (with 191 envelopes). For each grid resolution, the PL ratio was computed from equation (20) and the results were plotted in Figure 6. The integrity allocation was held constant (at 10^{-9}).

The grid resolution of the baseline distribution is intentionally low, to simplify validation and to enhance PL computation efficiency. However, significant excess inflation is the consequence of low resolution. With enhanced resolution, as illustrated in Figure 6, this excess inflation quickly disappears. The vast majority of excess inflation is

eliminated by doubling the grid resolution (from "1x" to "2x"). Further resolution doubling has a relatively minor impact on excess inflation. It can be inferred that the highest resolution case considered (the "8x" case) is very nearly converged to the continuum result. Convergence is evidenced toward the right side of the figure, where the convolved NavDEN PL ratio curve (ξ) approaches the biased-Gaussian PL ratio curve (ξ_{ref}), given by equation 22.

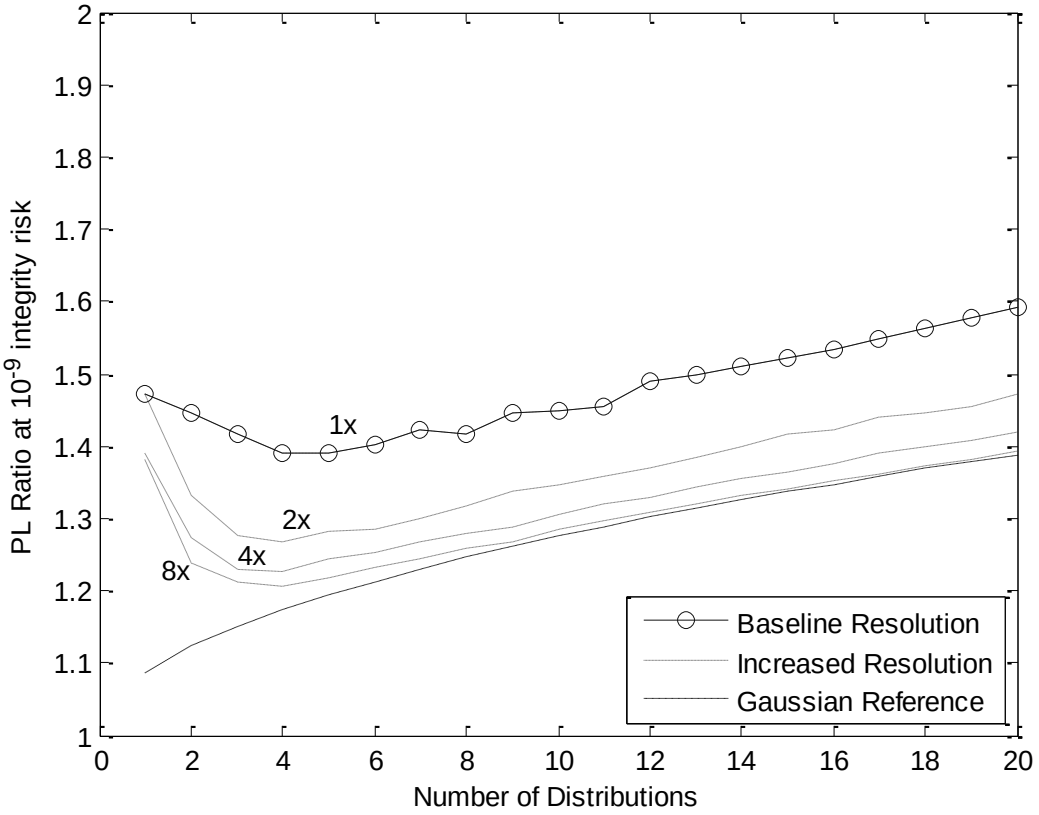

Figure 6. PL Ratio (for NavDEN as compared to Gaussian of same sigma) for a range of grid resolutions

The availability of satellite navigation often depends on establishing a tight integrity bound, with minimal excess inflation. Accordingly, we suggest that a reasonable tradeoff between computation, communication, and validation requirements can be achieved by using a NavDEN resolution at the "2x" grid resolution level (with 47 envelopes).

A topic for future work will be enhancing the efficiency of computing a PL using NavDEN models. Multiple discrete convolution operations are somewhat processor intensive for conventional avionics. Even at a moderate grid resolution (e.g. "2x" resolution), PL processing requirements for a NavDEN model are much larger than those for a conventional or biased-Gaussian model. Specifically, each convolution operation requires approximately M^2 operations (where M is the number of envelopes in the distribution). Thus, the total processor load to evaluate the PL is approximately M^2 larger for a NavDEN than for a conventional Gaussian.

VI. Application to Relevant Data Set

This section applies the NavDEN model to a GPS data set with heavier-than-Gaussian tails. The particular data set is a collection of error values (thermal noise and multipath) measured at the Federal Aviation Administration Technical Center (FAATC) to characterize a multipath-limiting antenna designed for use with the Ground Based Augmentation System (GBAS) for GPS [14]. Though the error distribution is very nearly Gaussian at its core, the NavDEN must flare to bound the data set's unusually heavy tails (requiring an alternative set of NavDEN parameters to those given previously, in Table 1). The FAATC data are illustrated on quantile axes in Figure 7 (individual dots).

The FAATC data set consists of 36 populations of error values for different satellite elevations (compiled in 1° bins from 4° to 39° elevation). Data samples were collected over a period of 72 days. The error values for each elevation bin have been normalized by their standard deviation. Most of the data points fall near the unit-variance Gaussian CDF, which appears as a straight (dotted) line on the quantile plot. Toward the edges of the plot, the empirical CDFs flare outward from this reference Gaussian. This flaring effect represents both a non-Gaussian probability of large errors and also uncertainty due to the relatively small number of data points available in the tails. To account for this uncertainty, a 95% confidence bounds was computed for each empirical CDF using the binomial distribution [31]; the bounding contour for these confidence bounds is plotted in Figure 7 as a dashed line.

Two distribution models were compared as alternatives for bounding the FAATC data. The first model was a paired Gaussian bound, consisting of two discretized Gaussian contours offset to the left and right, and the second model was a NavDEN. As paired bounds, both models can conservatively represent independent data sets of arbitrary distribution shape [11]. Parameters for each model were selected to provide a bound out to the edge of the data set and its associated 95% confidence bounds. The parameters of the NavDEN are summarized in Table 3.

The paired Gaussian has an inflated standard deviation, of 1.5σ, where σ is the nominal distribution standard deviation, and an offset of 0.68σ. As a comparison, an unbiased, continuous Gaussian would need to be inflated to a standard deviation of 2.0σ to bound the outermost points of the empirical CDF.

Table 3: NavDEN Parameters for FAATC Data

Parameter	Value
$\Delta_i / (S_i \sigma_i)$	**0.25**
$\tilde{x}_{\max}$	**32**
$\tilde{x}_{\min}$	**-32**
$\tilde{B}$	**28.6**
$\tilde{C}$	**57.2**
k_{tr}	**6**
k_{max}	**12**
$k_{\min}$	**-12**
k_{bias}	**1**

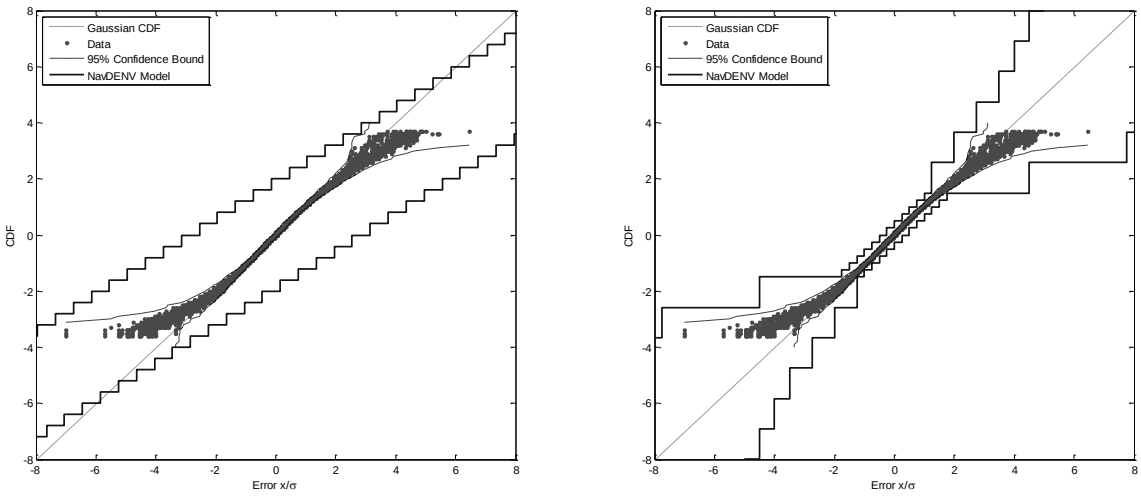

Figure 7. Paired Gaussian (left) and NavDEN Models (right) for a GPS Data Set

The NavDEN distribution provides a tight bound in the distribution core, where the data are approximately Gaussian distributed, and a loose fit for the far tails, where the data flare outward. Though the amount of flare required beyond the outer data points is speculative, it is evident that the NavDEN distribution provides substantially greater margin for uncertainty than the paired Gaussian (see Figure 7). In fact, there is likely some over-conservatism in the tail bound, in that the NavDEN roughly extrapolates the contours of the 95% confidence bounds for the empirical CDF; in concept, if the tail model turns out to be overly conservative, it can be tightened at a later time (when supporting data become available) by shrinking the flare parameters *B* and *C*.

Even though the NavDEN provides substantially more margin for uncertainty in the tails than does the paired-Gaussian bound, the NavDEN actually results in a smaller protection level when multiple error sources are combined. The reason is that, after multiple convolutions, the core distribution begins to dominate over the far tails. The core of the NavDEN is a much tighter representation of the actual data than the core of the paired Gaussian. Hence after as few as two IID convolutions, for an integrity allocation of 10^{-6}, the NavDEN distribution protection level is smaller than that of the paired Gaussian (see Figure 8). Even for an integrity allocation of 10^{-12}, the NavDEN outperforms the paired Gaussian for as few as five IID convolutions. Moreover, adverse effects associated with introducing a bias (e.g, worsening PL ratio at the right of Figure 5) are delayed because the bias is very small ($\Delta_i / S_i\sigma_i = 0.25$) compared to the far-tail splay. In fact, the PL ratio does not reach its minimum until well beyond the right edge of Figure 8, when *N* reaches a value of 22 for the 10^{-6} integrity allocation (and at even higher values of *N* for smaller integrity allocations). Since this bias penalty is delayed, the NavDEN inflation factor drops substantially as the number of convolved distributions grows large. In fact, it is worth noting that the PL inflation for the NavDEN drops below that associated with a traditional Gaussian (continuous, unbiased single-bound), which as noted earlier, has an inflated standard deviation of 2.0σ. The point where the NavDEN outperforms the traditional Gaussian occurs after three convolutions for an integrity of 10^{-6}, six for 10^{-9}, and ten for 10^{-12}. The NavDEN inflation continues to fall with a greater number of convolutions, dropping as low as 1.7 for all three integrity allocations.

In short, the NavDEN model features generally tighter protection levels than more conventional Gaussian-based models, while also providing greater margin for tail uncertainty. The NavDEN accomplishes both these

functions while maintaining a rigorous paired bound formulation, which has been proven to ensure conservative modeling of linear combinations of errors with arbitrary-shaped, independent distributions [11].

The fact that the NavDEN bound is rigorous, yet that its protection levels are relatively insensitive to heavily flared distribution tails, offers great potential to streamline the certification of new safety-of-life navigation systems. For example, it may be possible to reduce greatly the number of samples needed for certification if error-distribution tails can be extrapolated from a smaller data set (using extreme value theory or a consensus of experts). The extrapolated far-tail model would be necessarily uncertain, and its confidence bounds highly flared. The NavDEN can bound arbitrary tail flare while maintaining a tight Gaussian bound in the core. Thus, the NavDEN model is well suited to bound uncertain, extrapolated distribution tails.

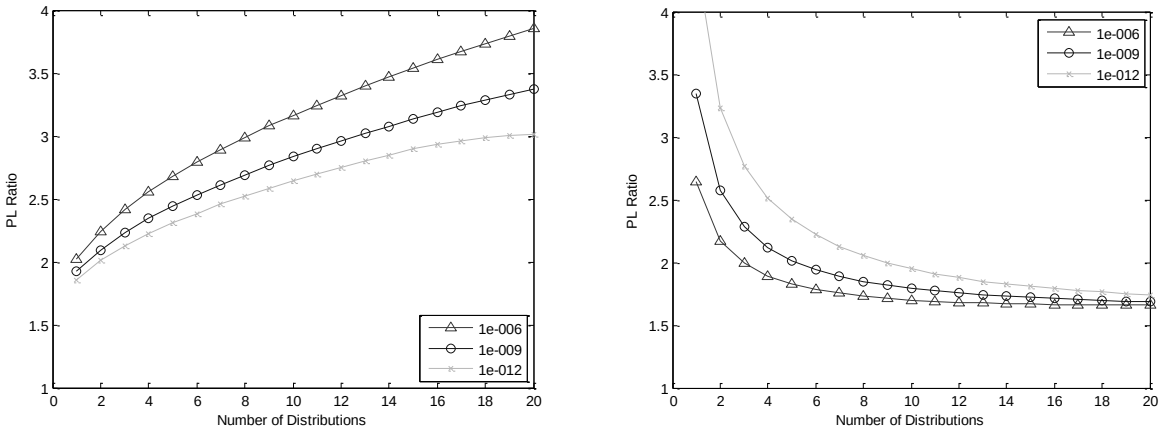

Figure 8. Width of integrity bound for Paired Gaussian (left) and NavDEN (right) models for a GPS data set, for case in which multiple IIDs are convolved

VII. Summary and Conclusions

A discrete error model, called the NavDEN, was introduced to overbound GNSS position-error distributions, which are not necessarily Gaussian. Whereas the NavDEN is Gaussian in its core, the distribution flares dramatically in its tails. A clear benefit of using NavDEN distributions is that it is possible to introduce rigorous bounds for uncertain distribution tails and to adapt those bounds as more sample data becomes available.

The NavDEN is customized for GNSS augmentation applications with aggressive requirements for validation, communication, and computation. The discrete structure of the NavDEN streamlines empirical validation. The

NavDEN also promotes efficient communication over band-limited channels, such as those used in existing GNSS augmentation systems; specifically, the NavDEN can be used with existing message structures that broadcast a single parameter for each error source. Also, the relatively coarse discretization of the NavDEN promotes efficient computation of a protection level, via a series of discrete convolution operations.

Analysis indicates that the effects of heavy-tails can be significantly mitigated, under typical circumstances, when NavDEN distributions are convolved together to evaluate protection level. Computing this convolution requires more processing than is required for a purely Gaussian-based protection level. However, in comparison to the more conventional approach of single-Gaussian or paired-Gaussian bounding, the NavDEN approach results in generally tighter protection levels when several error sources of similar magnitude are convolved, while also, remarkably, providing greater margin for bounding heavy and/or uncertain far tails of an empirical error distribution.

REFERENCES

[1] Joint Program and Development Office (JPDO). *Integrated Work Plan for the Next Generation Air Transportation System Version 1.0*, September 2008. http://www.jpdo.gov/iwp.asp

[2] SESAR Consortium. *SESAR Master Plan*, April 2008. http://www.eurocontrol.int/sesar/gallery/content/public/docs/European%20ATM%20Master%20Plan.pdf

[3] Erzberger, H. Transforming the NAS: The Next Generation Air Traffic Control System. In *Proceedings of the International Congress of the Aeronautical Sciences (ICAS)*, 2004.

[4] van Gool, M., and Schroter, H. PHARE Final Report. *PHARE Report DOC 99-70-09*, 1999. http://www.eurocontrol.int/phare/gallery/content/public/documents/99-70-09pharefinal10.pdf

[5] Rife, J., and Pullen, S. Aviation Applications. *GNSS Applications and Methods*, S. Gleason and D. Gebre-Egziabher, Eds., Artech House, 2009.

[6] Murphy, T., and Imrich, T. Implementation and Operational Use of Ground-Based Augmentation Systems (GBAS) – A Component of the Future Air Traffic Management System. *Proceedings of the IEEE*, 2008, **96**, 12, 1936-1957.

[7] Braff, R., and Shively, C. A Method of Over Bounding Ground Based Augmentation System (GBAS) Heavy Tail Error Distributions. *Journal of Navigation*, 2005, **58**, 1, 83-103.

[8] Lee. J., Pullen, S., and Enge, P. Sigma Overbounding using a Position Domain Method for the Local Area

Augmentation of GPS. *IEEE Transactions on Aerospace and Electronic Systems*, 2009, **45**, 4, 1262-1274.

[9] Rife, J., Pullen, S., and Pervan, B. Core Overbounding and its Implications for LAAS Integrity. In *Proceedings of the ION-GNSS*, 2004, 2810-2821.

[10] Walter, T., Blanch, J., and Enge, P. Evaluation of Signal in Space Error Bounds to Support Aviation Integrity. *NAVIGATION*, 2010, 57, 2, 101-113.

[11] Rife, J., Pullen, S., Pervan, B., and Enge, P. Paired Overbounding for Nonideal LAAS and WAAS Error Distributions. *IEEE Transactions on Aerospace and Electronic Systems*, 2006, **42**, 4, 1386-1395.

[12] DeCleene, B. Defining Pseudorange Integrity – Overbounding. In *Proceedings of the ION-GPS*, 2000, 1916-1924.

[13] Walter, T., Blanch, J., and Rife, J. Treatment of Biased Error Distributions in SBAS. *Journal of Global Positioning Systems*, 2004, **3**, 1-2, 265-272.

[14] Warburton, J. *LGF Sigma Pseudorange Ground Establishment, Overbounding and Monitoring: Support Data*. Presented by the FAA William J. Hughes Technical Center to RTCA SC-159, 2002.

[15] Williamson, R.C., and Downs, T. Probabilistic Arithmetic. I. Numerical Methods for Calculating Convolution and Dependency Bounds. *International Journal of Approximate Reasoning*, 1990, **4**, 2, 89-158.

[16] Tonon, F., Bernardini, A., and Mammino, A. Reliability Analysis of Rock Mass Response by Means of Random Set Theory. *Reliability Engineering & System Safety*, 2000, **70**, 3, 263-282.

[17] Berleant, D., Xie, L., Zhang, J. Statool: A Tool for Distribution Envelope Determination (DEnv), an Interval-Based Algorithm for Arithmetic on Random Variables. *Reliable Computing*, 2003, **9**, 2, 1385-3139.

[18] Berleant, D. and Zhang, J. Using Pearson Correlation to Improve Envelopes around the Distributions of Functions. *Reliable Computing*, 2004, **10**, 2, 1385-3139.

[19] Rife, J., and Gebre-Egziabher, D. Symmetric Overbounding of Correlated Errors. *NAVIGATION*, 2007, **54**, 2, 109-124.

[20] Pulford, G. A Proof of the Spherically Symmetric Overbounding Theorem for Linear Systems. *NAVIGATION*, 2008, **55**, 4, 283-292.

[21] Pervan, B., and Sayim, I. Sigma Inflation for the Local Area Augmentation of GPS. *IEEE Transactions on Aerospace and Electronic Systems*, 2001, **37**, 4, 1301-1311.

[22] Rife, J., Walter, T., and Blanch, J. Overbounding SBAS and GBAS Error Distributions with Excess-Mass

Functions. In *Proceedings of IGNSS*, 2004.

[23] Raytheon. *Algorithm Contribution to HMI for the Wide Area Augmentation System*. Raytheon Company Unpublished Work, 2002.

[24] Azais, J-M., Gadat, S., Lévy, J-C., Rols, B., Mercadier, C., Jordan, C., Suard, N. GNSS Integrity Achievement by using Extreme Value Theory. In *Proceedings of the ION-GNSS*, 2009, 1281-1287.

[25] RTCA Inc., *Minimum Operational Performance Standards for GPS/Wide Area Augmentation System Airborne Equipment*. RTCA/DO-229D, 2006.

[26] RTCA Inc., *GNSS-Based Precision Approach Local Area Augmentation System (LAAS) Signal-in-Space Interface Control Document (ICD)*. RTCA/DO-246B, 2001.

[27] Misra, P., and Enge, P. *Global Position System: Signals, Measurements, and Performance*. Ganga-Jamuna Press, 2006.

[28] Shively, C., and Hsiao, T. Availability Enhancements for Cat IIIB LAAS. *NAVIGATION*, 2004, **51**, 1, 45-58.

[29] Rife, J., and Pullen, S. The Impact of Measurement Biases on Availability for Category III LAAS. *NAVIGATION*, 2005, **52**, 4, 215-228.

[30] Xie, G., Pullen, S., Luo, M., Normark, P-L., Akos, D., Lee, J., and Enge, P. Integrity Design and Updated Test Results for the Stanford LAAS Integrity Monitor Testbed. In *Proceedings of ION Annual Meeting*, 2001, 681-693.

[31] Wright, T. *Exact Confidence Bounds when Sampling from Small Finite Universes : an Easy Reference Based on the Hypergeometric Distribution*. Springer-Verlag, 1991.

Jason Rife (M'01) received his B.S. degree in mechanical and aerospace engineering from Cornell University, Ithaca, NY, in 1996, and his M.S. and Ph.D. degrees in mechanical engineering from Stanford University, Stanford, CA, in 1999 and 2004.

He is currently an Assistant Professor of Mechanical Engineering at Tufts University in Medford, Massachusetts. At Tufts, he directs the Automation Safety and Robotics Laboratory (ASAR), which applies theory and experiment to characterize the integrity of autonomous vehicle systems. Previously, after completion of his graduate studies, he worked as a researcher with the Stanford University GPS Laboratory, serving as a member of the Local Area Augmentation System (LAAS) and Joint Precision Approach and Landing System (JPALS) teams.

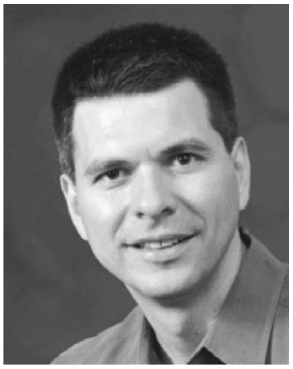

Boris Pervan received a B.S. from the University of Notre Dame in 1986, M.S. from the California Institute of Technology in 1987, and Ph.D. from Stanford University in 1996, all in aerospace engineering.

From 1987 to 1990, he was a systems engineer at Hughes Space and Communications Group responsible for mission analysis on commercial and government spacecraft programs. He was a research associate at Stanford from 1996 to 1998, serving as project leader for GPS Local Area Augmentation System (LAAS) research and development. He is now an Associate Professor of Mechanical and Aerospace Engineering at the Illinois Institute of Technology (IIT) in Chicago.

Dr. Pervan received the RTCA William E. Jackson Award (1996), the M. Barry Carlton Award from the IEEE Aerospace and Electronic Systems Society (1999), Sigma Xi Outstanding Research Award at IIT (2005), Excellence in Teaching awards at IIT (2002, 2005), the Albert Zahm Prize in Aeronautics at Notre Dame (1986), and the Guggenheim Fellowship at Caltech (1987). He is currently editor of the ION journal Navigation.